BIBLIOGRAPHY

1. G. A. Barnard and T. Bayes, Studies in the history of probability and statistics: IX. Thomas Bayes's essay toward solving a problem in the doctrine of chances. *Biometrika*. 1958; **45**(3/4):293–315.
2. R. T. Cox, Probability, frequency, and reasonable expectation. *Am. J. Phys*. 1946; **14**:1–13.
3. E. T. Jaynes, *Probability Theory: The Logic of Science*. Cambridge, U.K.: Cambridge University Press, 2003.
4. R. A. Howard, Decision analysis: Perspectives on inference, decision, and experimentation. *Proc. IEE*. 1970; **58**(5):823–834.
5. D. von Winterfeldt and W. Edwards, *Decision Analysis and Behavioral Research*. Cambridge, U.K.: Cambridge University Press, 1986.
6. D.V. Lindley, A statistical paradox. *Biometrika*. 1957; **44**: 187–192.
7. P. M. Lee, *Bayesian Statistics: An Introduction*. London: Edward Arnold, 1989.

BIOACOUSTIC SIGNALS

LEONTIOS J. HADJILEONTIADIS
STAVROS M. PANAS
Aristotle University of Thessaloniki
Thessaloniki, Greece
IOANNIS T. REKANOS
Technological and Educational Institute of Serres
Serres, Greece

1. INTRODUCTION

Bioacoustic signals (BAS) are defined as a family of signals that includes the sounds produced by the human body, whereas, in general, the study of sounds produced by living organisms is referred to as bioacoustics (1). As BAS are the audible outcome emitted from the human body, they possess valuable diagnostic information regarding the functionality of the human organs involved in the sound production mechanisms.

An everyday-life example of BAS is the pressure signals produced from the beating of the heart, namely heart sounds (HS). To obtain HS, a stethoscope is typically placed on the chest above the heart. The end of the stethoscope has a diaphragm that bends in response to sound; the sound waves travel through the tubes of the stethoscope to the clinician's ears. The clinician listens to these sounds to determine certain aspects of the mechanical functioning of the heart (mostly whether the heart valves are functioning properly or not), of which the clinician has been trained to detect. This measurement is qualitative. A microphone can also be used to pick up sound. Microphones convert the mechanical energy of sound into electric energy. The resulting analog electric signal can be digitized and analyzed quantitatively with computer-based algorithms. Consequently, proper extraction and use of the diagnostic information of the digitized BAS can transform the art of BAS auscultation into a scientific discipline. With proper signal processing methods, the BAS could be converted from acoustic vibrations inside the human organism into graphs and parameters with diagnostic value, resulting in novel diagnostic tools that objectively track the characteristics of the relevant pathology and assist the clinicians in everyday practice.

Apart from HS, the BAS family also includes lung sounds (LS), bowel sounds (BS), and joint sounds (JS), with LS and HS being the most often used BAS in everyday clinical practice, although, recently, sufficient research effort has been placed on BS and JS analysis, facilitating their adoption by the physicians as diagnostic means.

2. DEFINITION, CATEGORIZATION, AND MAIN CHARACTERISTICS OF BAS

2.1. Lung Sounds

2.1.1. Definition and Historical Background. From the time of ancient Greeks and their doctrine of medical experimentation until at least the 1950s, the LS were considered as *the sounds originating from within the thorax* and they were justified mainly on the basis of their acoustic impression. For example, the writings of the Hippocratic School, in about 400 B.C., describe the chest (lung) sounds as splashing, crackling, wheezing, and bubbling sounds emanating from the chest (2). An important contribution to the qualitative appreciation of LS and HS was the invention of the stethoscope by René Theophil Laënnec in 1816. Laënnec's gadget, which was originally made of wood, replaced the "ear-upon-chest" detection procedure enhancing the emitted LS and HS (3). Unfortunately, it took over a century for quantitative analysis to appear. Attempts for a quantitative approach date to 1930, but the first systematic, quantitative measurement of their characteristics (i.e., amplitude, pitch, duration, and timing in controls and in patients) is attributed to McKusick et al., in 1953 (4); the door to the acoustic studies in medicine was finally opened.

2.1.2. Categorization and Main Characteristics. The LS are divided into two main categories [i.e., *normal* LS (NLS) and *abnormal* LS (ALS)]. The NLS are certain sounds heard over specific locations of the chest during breathing in healthy subjects. The character of the NLS and the location at which they are heard defines them. Hence, the category of the NLS includes the following types (5):

- *tracheal* LS (TLS), heard over the trachea having a high loudness,
- *vesicular* LS (VLS), heard over dependent portions of the chest, not in immediate proximity to the central airways,
- *bronchial* LS (BLS), heard in the immediate vicinity of central airways, but principally over the trachea and larynx,

– *bronchovesicular* LS (BVLS), which refers to NLS with a character in between VLS and BLS heard at intermediate locations between the lung and the large airways, and
– *normal crackles* (NC), inspiratory LS heard over the anterior or the posterior lung bases (6,7).

The ALS consist of LS of a BLS or BVLS nature that appear at typical locations (where VLS are the norm). The ALS are categorized between *continuous adventitious sounds* (CAS) and *discontinuous adventitious sounds* (DAS) (8), and include the following types (9–11):

– *wheezes* (WZ), musical CAS that occur mainly in expiration and invariably associated with airway obstruction, either focal or general,
– *rhonchi* (RH), low-pitched sometimes musical CAS that occur predominantly in expiration, associated more with chronic bronchitis and bronchiectasis than with asthma,
– *stridors* (STR), musical CAS that are caused by a partial obstruction in a central airway, usually at or near the larynx,
– *crackles*, discrete, explosive, nonmusical DAS, further categorized between:

• *fine crackles* (FC), high-pitched exclusively inspiratory events that tend to occur in mid-to-late inspiration, repeat in similar patterns over subsequent breaths and have a quality similar to the sound made by strips of Velcro being slowly pulled apart; they result from the explosive reopening of small airways that had closed during the previous expiration, and
• *coarse crackles* (CC), low-pitched sound events found in early inspiration and occasionally in expiration as well, develop from fluid in small airways, are of a "popping" quality, and tend to be less reproducible than the FC from breath to breath,

– *squawks* (SQ), short, inspiratory wheezes that usually appear in allergic alveolitis and interstitial fibrosis (12), predominantly initiated with a crackle, caused by the explosive opening and fluttering of the unstable airway that causes the short wheeze, and
– *friction rub* (FR), DAS localized to the area overlying the involved pleura and occur in inspiration and expiration when roughened pleural surfaces rub together, instead of gliding smoothly and silently.

As the preceding paragraph has demonstrated, it is not difficult to provide evidence that the LS are directly related to the condition of the pulmonary function. The variety in the categorization of LS implies changes in the acoustic characteristics either of the source or the transmission path of the LS inside the lungs because of the effect of a certain pulmonary pathology. It is likely that the time- and frequency-domain characteristics of the LS signals reflect these anatomical changes (13).

In particular, the time-domain pattern of the NLS resembles a noise pattern bound by an envelope, which is a function of the flow rate (13). Tracheal sounds have higher intensity and a wider frequency band (0–2 kHz) than the chest wall sounds (0–600 Hz) and contain more acoustic energy at higher frequencies (14). The CAS time-domain pattern is a periodic wave that may be either sinusoidal or a set of more complex, repetitive sound structures (13). In the case of WZ, the power spectrum contains several peaks ("polyphonic" WZ), or a single peak ("monophonic" WZ), usually in the frequency band of 200–800 Hz, indicating bronchial obstruction (13). Crackles have an explosive time-domain pattern, with a rapid onset and short duration (13). It should be noted that this waveform may be an artifact of high-pass filtering (15). Their time-domain structural characteristics (i.e., a sharp, sudden deflection usually followed by a wave) provide a means for their categorization between FC and CC (16), as it is shown in Fig. 1.

For an extensive description and a variety of examples regarding the LS structure and characteristics, the reader should refer to (13).

2.2. Heart Sounds

2.2.1. Definition and Historical Background. HS are defined as *the repetitive "lub-dub" sounds of the beating of the heart* (17). Heart auscultation followed similar pathways with lung auscultation because of the topological coexistence of the heart with lungs. Hippocrates (460–377 B.C.) was familiarized with heart auscultation, and he may have used HS for diagnostic purposes (18). Nevertheless, it took almost two thousand years for re-evaluation of HS by William Harvey (1578–1657), and three hundred years more, with the contribution of Laënnec's stethoscope (1816), for Dr. Joseph Skoda (1805–1881) first to describe the cardiac sounds and murmurs, by pinpointing their locations and defining the clinical auscultatory signs that have allowed the noninvasive diagnosis of cardiac pathology via auscultation (18).

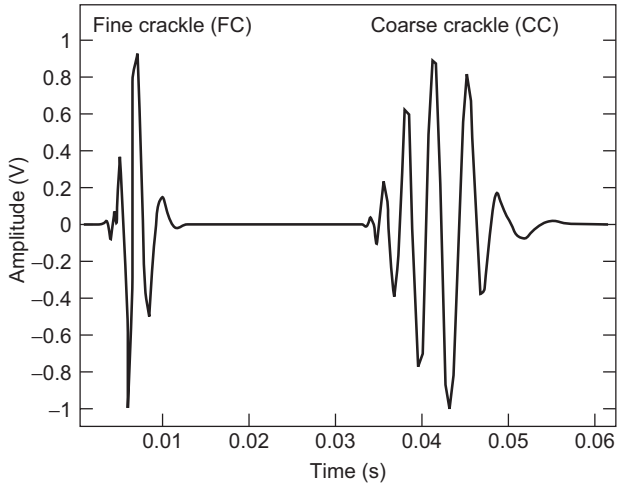

Figure 1. An example of the crackles morphology in the time-domain used for their categorization into fine and coarse crackles.

2.2.2. Categorization and Main Characteristics. The HS are named according to their sequence of occurrence and are originated at specific points in the cardiac cycle (18). In particular, the HS are categorized as follows:

– *first heart sound*, or S_1, occurs at the beginning of ventricular systole when ventricular volume is maximal and is considered as normal HS,
– *second heart sound*, or S_2, occurs at the end of ventricular systole and is considered as normal HS too,
– *third heart sound*, or S_3 or "S_3 gallop," occurs just after the S_2, as a result of decreased ventricular compliance or increased ventricular diastolic volume, and is a sign of congestive heart failure,
– *fourth heart sound*, or S_4 or "S_4 gallop," occurs just before the S_1, as a result of decreased ventricular compliance or increased volume of filling, and is a sign of ventricular stress, and
– *murmurs*, sustained noises that are audible during the time periods of systole, diastole, or both, associated with backward regurgitation, forward flow through narrowed or deformed valve, a high rate of blood flow through normal or abnormal valves, vibration of loose structures within the heart (chordaetendineae), and continuous flow through A-V shunts. They are further categorized between:

• *systolic murmurs* (SM), sustained noises that are audible between S_1 and S_2, categorized as *early* SM, which begin with S_1 and peak in the first third of systole; *mid* SM (or "ejection" murmur), which begin shortly after S_1, peak in mid-systole, and do not quite extend to S_2; *late* SM, which begin in the later one-half of systole, peak in the later third of systole, and extend to S_2; and *pansystolic murmurs*, which begin with S_1 and end with S_2, thus heard continuously at about constant amplitude throughout systole, and
• *diastolic murmurs* (DM), sustained noises that are audible between S_2 and the next S_1, categorized as *early* DM, which begin with S_2 and peak in the first third of diastole; *mid* DM, which begin after S_2 and peak in mid-diastole; *late* DM, which begin in the latter one-half of diastole, peak in the later third of diastole, and extend to S_1; and *pandiastolic murmurs*, which begin with S_2 and extend throughout the diastolic period.

The acoustic content of HS is concentrated in low frequencies (19). In fact, over 95% of the acoustic energy of S_1 and 99% of the one of S_2 is concentrated under the 75 Hz (20). The average spectrum decays exponentially from its peak at approximately 7 Hz and often contains one or more shallow and wide peaks (21). The S_2 contains much more energy in the lower frequencies than S_1 does. In addition, the frequency content of most cardiac murmurs is also in the low range (20). The two most common HS (i.e., S_1, and S_2) have much longer duration and thus a lower pitch than crackles, and both of them are short-lived compared with NLS and CAS (17), which contributes to the facilitation of their separation from the LS. Nevertheless, HS from patients with irregular cardiac rhythms (transient character) or loud murmurs tend to overlap the LS more and thus are less separable.

2.3. Bowel Sounds

2.3.1. Definition and Historical Background. Bowel sounds are defined as *the sounds heard when contractions of the lower intestines propel contents forward* (22). Knowledge of BS has advanced little since Cannon's pioneering work in 1902 (23), which used the sounds as a way of studying the mechanical activity of the gastrointestinal tract. Clinical tradition assesses the BS in a "passive" way (i.e., by tracing not their presence but their absence) because the latter is an indicator of intestinal obstruction or ileus (paralysis of the bowel) (22). This lack of interest in "active" abdominal auscultation is due, in part, to its lack of support in scientific fact and definitely not because of its lack of diagnostic information. Bowel sound patterns in normal people have not been clearly defined, as only a small number of them have been studied (24–28). In addition, the trivial signal processing methods that have been involved (29–31) have also been a problem. The vague notion about the usefulness of the BS in clinical practice that has been cultivated all these years, along with the lack of a worldwide-accepted BS categorization, has resulted in a reduced interest in their processing and evaluation, even today.

2.3.2. Categorization and Main Characteristics. Up to now, no reference of what can be considered as normal bowel sound activity, and no physiological understanding of the significance of different types of BS exist. Attempts to describe the acoustic impression of normal BS, such as "rushes," "gurgles," etc., fail because of their subjectivity bias. Sporadic works in the literature try to analyze the time- and frequency-domain characteristics of BS, defining as normal BS those with a frequency content in the range of 100–1000 Hz, with durations within a range of 5–200 msec, and with widely varying amplitudes (32). An analysis of the "staccato pop," which is one of the most common BS characteristic of the colon, proves that it has a frequency content between 500 and 700 Hz and a duration of 5 to 20 msec (32).

Recent work based on the differences seen between the sound-to-sound intervals of BS from different pathologies (i.e., irritable bowel syndrome, Crohn's disease, and controls) introduces a time-domain-based tool for relating BS to the associated bowel pathology (33). In a similar vein, the approaches of BS presented in this chapter contribute to the provision of an extended, accurate, and objective alternative to the current BS processing and evaluation status.

2.4. Joint Sounds

2.4.1. Definition and Historical Background. JS are defined as the sounds heard during the functioning of a joint. In particular, the sound heard when our knuckles crack results when a finger joint is extended almost to the end of its range. The joint, surrounded by a lubricating fluid, is encased in a capsule. At times, we intentionally or

unintentionally extend the joint so far that the gas dissolved in the fluid spontaneously separates from the solution, forming a small bubble, and making a cracking sound. Not until the fluid reabsorbs the gas can the sound be reproduced. On the other hand, the sound heard when we do deep-knee bends is a snapping sound, produced when our tendons, which are merely the fibers that connect muscles and bones, elastically snap into new positions as our joints move under stress. Because the tendons shift back and forth with the movement of the joint, no waiting time exists before this snapping sound can be reproduced.

Another interesting joint that produces JS is the temporomandibular (jaw) joint (TMJ), which is the "ball and socket" joint that allows the lower jaw to open, close, and move sideways when chewing and speaking. Located about one centimeter in front of the ears, they are the only joints in the head. The ball is technically known as the "condyle" of the joint, and it rotates in a cuplike depression (the socket) technically known as the "fossa." Although the joint looks like it is attached directly to the sinuses, it is actually separated from them by soft tissue ligaments that entirely enclose the joint. The "meniscus" is a disk of cartilage that lives in the space between the condyle and the fossa and is capable of moving forward and backward as the jaw opens and closes. The condyle and the fossa are each covered with a thin layer of nonmovable cartilage of their own. All three layers of cartilage help to provide smooth, frictionless surfaces for comfortable joint operation. TMJ sounds (TMJS) are produced in the form of clicking or crepitation. In many cases, the cartilage that separates the ball from the socket tends to tear and displace so that it bunches up in front of the ball. When opening the jaw wide, the ball moves forward pushing the bunched up cartilage in front of it. At some point in this forward movement, the ball jumps over the mass of cartilage snapping back hard onto the bone on the other side causing a loud pop or clicking sound. Sometimes, the bones are forced into such close approximation that you might hear a grinding noise (crepitus) when opening or closing (34).

Robert Hooke is credited with the first auscultation of a joint in the Seventeenth century and for the first suggestion that joint noises could be used as diagnostic sign in patients suffering from painful joints. Heuter described, in 1885, a "myo-dermato-osteophone" to localize loose bodies in joints (35). In 1902, Blodgett reported on auscultation of the knee, with attention to sounds of apparently normal joints, the change in sounds with repetitive motions, and reproducibility over several days (36). He notes an age-related increase of sound and the relative absence of sound when an effusion was present. Bicher, in 1913, reported that each type of meniscal injury emitted a distinctive sound signal (37). A paper on the *Value of Joint Auscultation* was published in 1929 by Walters, in which joint sounds recorded from 1600 patients were graded and correlated with presumed pathology (38). The results were said to help in the diagnosis of painful joints, with limited physical findings and normal "skiagrams." These studies were expanded by Erb, who used a contact microphone to reduce extraneous sounds (39). His was the first attempt at electronic and graphic recording of the knee joint sound (KJS) signal. A "cardiophone" was used by Steindel to listen to sounds at several locations (40), and he appears to be the first to have recorded joint angles and the first to include filtering to remove noise and improve the signal. He classified the JS based on the pitch, amplitude, and sequence of the sounds, which in many cases were correlated with pathology demonstrated by operative findings. In 1953, Peylan reported on a study of 214 patients with several types of arthritis using a regular and an electronic stethoscope (41). He believed that he could distinguish between periarticular sounds, osteoarthritis, and rheumatoid arthritis, but did not present evidence of any "blind" evaluation of this ability. Fischer and Johnson showed, in 1960, that sound signals could be detected in rheumatoid arthritis before x-ray changes were observable (42). Chu et al. at Ohio began the true scientific analysis of JS in a series of papers dealing with methods to reduce skin friction and ambient noise; the use of statistical parameters, such as the autocorrelation function of the KJS signal for classification of signals into categories, such as rheumatoid arthritis, degenerative arthritis, and chondromalacia patella; and the relationship between signal acoustic power and articular cartilage damage (surface roughness) (43,44). They also pointed to a number of artifacts (local and ambient) in the acoustic recording of KJS. A good understanding of the nature of the KJS signals, their diagnostic potentials, as well as the problems encountered in practice may be obtained from the work of Mollan et al. in Northern Ireland (45–49).

2.4.2. Categorization and Main Characteristics. From the aforementioned JS, the TMJS and KJS are the most important aspects. According to Widmalm et al. (50), the TMJS are categorized in five types of clicking, i.e.,:

- *Types* 1, 2, *and* 3: short-duration signals with well localization in the time-frequency domain with a single energy peak in the frequency range below 600 Hz, from 600 Hz to 1200 Hz, and above 1200 Hz, respectively.
- *Types* 4 *and* 5: long-duration crepitation signals with nonlocalization in the time-frequency domain. Type 4 sounds contain all of the energy in the frequency region below 600 Hz, whereas type 5 sounds have energy both below 600 Hz and above 600 Hz.

Similar to the case of BS, the categorization of KJS is implied through the related knee pathology. As Mollan et al. note (49), patients with meniscal injuries produce characteristic KJS signals, and that alterations in normal joint crepitus may be a useful indicator of early cartilage degeneration. They report the largest KJS signal on the affected side, with a large displacement, and repetitive appearance at the same knee angle in cycles. In addition, bizarre, irregular KJS signals are noticable in the range of 300 Hz to 600 Hz, produced by degenerate articular cartilage. Furthermore, Frank et al. (51) report sharp bursts (click) in the KJS signal for the case of meniscal lesions, with short-duration energy in the range of 0–200 Hz. Mild chondromalacia (softening of the cartilaginous surface of

the inner side of the patella, namely the chondrol) is seen in the KJS signal as long-duration activity in the range of 0–300 Hz. Finally, KJS signals associated with severe chondromalacia are of relatively low frequencies (i.e., 0–100 Hz) because of loose cartilage tissue existing between the rubbing surfaces.

3. RECORDING STANDARDS OF BAS

3.1. Recording Sensor Types

The BAS auscultation is traditionally performed by means of the stethoscope. Listening to BAS by means of a stethoscope involves several physical phenomena, such as vibrations of the chest wall that are converted into pressure variations of the air in the stethoscope, and these pressure variations are then transmitted to the eardrum. However, the stethoscope cannot be used in the quantitative analysis of BAS, because it does not provide any means of signal recording. In addition, it presents a selective behavior in its frequency response instead of a flat one (at least in the area of interest, 40–4000 Hz).

One basic category of recording devices of BAS signals refers to microphones. Whatever the type of microphone, it always has a diaphragm, like in the human ear, and the movement of the diaphragm is converted into an electric signal. Two major microphone approaches exist: the "kinematic" approach, which involves the direct recording of chest-wall movement ("contact sensor") and the "acoustic" approach, which involves the recording of the movement of a diaphragm exposed to the pressure wave induced by the chest-wall movement ("air-coupled sensor"). The chest-wall movements are so weak that a free-field recording is not possible; it is essential to couple the diaphragm acoustically with the chest wall through a closed-air cavity. Whatever the approach, kinematic or acoustic, vibrations must be converted into electric signals using transduction principles of (52): electromagnetic induction (movement of a coil in a magnetic field induces an electric current through the coil); condenser principle (changing the distance between the two plates of a charged capacitor induces a voltage fluctuation); and piezoelectric effect [bending of a crystal (rod, foil) for the induction of an electric charge on the surface].

The other category of recording devices includes piezoelectric accelerometers. A piezoelectric accelerometer applies the piezoelectric effect in such a way that the output voltage is proportional to the acceleration of the whole sensor. Early applications used heavy-weight sensors with high sensitivity and good signal-to-noise ratio. The disadvantages because of its heavy mass are mechanical loading of the surface wall, difficulties with attachment, and a low resonance frequency (well within the band of interest). A piezoelectric accelerometer of very low mass (1 g) has been applied successfully in the past, yet it may be so fragile that routine clinical applications may be difficult (52).

Although both condenser microphones and piezoelectric contact sensors are displacement receivers, the waveforms that they deliver are different because of the coupling differences. Selection criteria of a device should also include size, average lifetime, and maintenance cost. Both sensors possess some disadvantages [i.e., piezoelectric sensors are very sensitive to movement artifacts, for example, by the connecting wire, their characteristics depend on the static pressure against the body surface (53) and they are brittle, whereas condenser microphones need mounting elements that change the overall characteristics of the sound transduction (52)].

3.2. Recording Procedures and Considerations

The most common bandwidth for LS is from 60–100 Hz to 2 kHz when recorded on the chest and from 60–100 Hz to 4 kHz when recorded over the trachea. In addition, recording of adventitious sounds on the chest requires a bandwidth from 60–100 Hz to 6 kHz (52). For HS, the useful bandwidth is from 20 Hz to 150 Hz, whereas for BS, the useful bandwidth is similar to the LS recorded from the chest (i.e. 60–2000 Hz). As a result, sampling frequencies of 5 kHz to 10 kHz and of 1 kHz to 2 kHz are sufficient enough for the acquisition of all LS and HS signals, respectively.

The KJS bandwidth is controversial, and different ranges have been reported in the literature. In particular, Chu et al. mention that the frequency content of the that KJS extends to 20 kHz (43,44) whereas Mollan's work indicates that the KJS signal is predominantly low-frequency in nature (45–49). They also point out the importance of the lower frequencies, which are missed by acoustic microphones but are recorded by contact sensors. The use of the latter obviates the need to record the KJS signals in an anechoic or soundproof chamber, or the need to employ a differential microphone pair for noise cancellation, as in Chu's experimental setup (43,44). Contact sensors are insensitive to background noise and small in size in order to be securely fixed to minimize skin friction (51). Furthermore, multiple sensors can be employed to localize defects by multichannel KJS signal analysis (49).

For the case of TMJS, recent studies (50,54) indicate that the analysis of TMJS needs to cover the whole audible range (from 20 Hz to 20 kHz). Consequently, sampling frequency of 48 kHz is the most preferable. Electret microphones, like the SONY ECM 77, have a flat frequency response from 40 Hz up to 20 kHz in free-space and are usually preferred in the recordings of almost all types of BAS.

For the processing of BAS, an analogue system is required, which consists of a sensor, an amplifier, and filters that condition the signal prior to analogue-to-digital (A/D) conversion (usually with a 12- or 16-bit resolution). A combination of low-pass filters (LPF) and high-pass filters (HPF) in cascade is usually applied. The purpose of using a HPF is to reduce the heart, muscle, and contact noises. The LPF is needed to eliminate aliasing. The amplifier is used to increase the amplitude of the captured signal so that the full A/D converter range can be optimally used, and sometimes to adjust the impedance of the sensor.

Table 1 tabulates the recommendations regarding the acquisition of the LS signals. These recommendations can easily be adapted to the rest of the BAS, taking into account the aforementioned characteristics per signal category.

Table 1. Summary of Recommendations for the Case of LS Signal Acquisition with Piezoelectric or Condenser Sensors.

Sensor specifications	
Frequency response	Flat in the frequency range of the sound. Maximum deviation allowed 6 dB
Dynamic range	>60 dB
Sensitivity	Must be independent of frequency, static pressure, and sound direction
Signal-to-noise ratio	>60 dB ($S = 1\,\text{mV} \cdot \text{Pa}^{-1}$)
Directional characteristics	Omnidirectional
Coupling	
Piezoelectric contact	
Condenser air-coupled	Shape: conical; depth: 2.5–5 mm; diameter at skin: 10–25 mm; vented
Fixing methods	
Piezoelectric	Adhesive ring
Condenser	Either elastic belt or adhesive ring
Noise and interferences	
Acoustic	Shielded microphones; protection from mechanical vibrations
Electromagnetic	Shielded twisted pair or coaxial cable
Amplifier	
Frequency response	Constant gain and linear phase in the band of interest
Dynamic range	>60dB
Noise	Less than that introduced by the sensor
High-pass filtering	Cut-off frequency 60 Hz; roll-off $>18\,\text{dB} \cdot \text{octave}^{-1}$; phase as linear as possible; minimized ripple
Low-pass filtering	Cut-off frequency above the upper frequency of the signal; roll-off $>24\,\text{dB} \cdot \text{octave}^{-1}$; minimized ripple

Source: Ref. 52.

4. BAS ANALYSIS

The original method of BAS interpretation is auscultation of the sound signals by the physician. Modern computer-based analysis extend BAS capabilities by supplying information not directly from the sound perception. Nevertheless, auscultation is still a widespread technique, because it involves the use of the stethoscope. To this end, in most cases, the agreement of an automatic method with physician's interpretation is a basic criterion for its acceptance.

The BAS analysis includes three main categories: noise reduction-detection, modeling, and feature extraction-classification.

4.1. Noise Reduction Detection

Objective analysis of BAS requires a preprocessing procedure regarding the elimination of possible noise effect in the recorded signal, which mainly refers to the elimination of the impact of the HS on the LS recordings, elimination of the background noise from BAS recordings or detection of BAS with transient character, such as DAS or BS bursts, and reduction of interference in different representations of BAS, like the TMJS or HS time-frequency representation. The above cases are met in the routine recordings of BAS; hence, advanced signal processing techniques are needed in order to efficiently circumvent these noise effects.

4.1.1. HS Interference Elimination. Heartbeating produces an intrusive quasi-periodic interference that masks the clinical auscultative interpretation of LS. This is a serious noise effect that creates major difficulties in LS analysis because of the fact that the intensity of HS is three- to ten-fold that of LS over the anterior chest and one- to three-fold that of LS from the posterior bases (55). This high relative intensity of the HS can easily saturate the analog amplifiers or the A/D converter, leading to a truncated signal and artifacts, especially in the case of children and infants, where the heart rate is high and its HS are loud (56,57). As it is already mentioned, the main frequency components of the HS are in the range of 20 Hz to 150 Hz (58,59) and overlap with the low-frequency components of breath sound spectrum in the range of 20 Hz to 2000 Hz (14).

Two basic approaches for heart noise reduction were followed in the literature: high-pass (HP) linear filtering, with a cutoff frequency varying from 50 Hz to 150 Hz, and adaptive filtering. The first approach (14,52) effectively reduces the HS noise, but, at the same time, it degrades the respectively overlapped frequency region of breath sounds. The second approach uses the theory of adaptive filtering (60) with a reference signal highly correlated to the noise component of the input signal. To this vein, a signal preprocessing system with varying amplifier gain using an adaptive filter (61) was initially proposed. In addition, a portable breath sound analysis system that uses an adaptive filter based on the Least Mean Square (LMS) algorithm for removing HS interferences (62) was suggested. In both cases, HS signals recorded on the patient's heart location were used as the reference input for adaptive filtering, which inevitably included LS as

well. Electrocardiogram (ECG) signal information was also used as the reference signal for LMS-based adaptive filtering to reduce HS (57,63), using hundreds of taps (i.e., 1000 and 300, respectively) resulted, however, in a high adaptation time. The use of reduced order Kalman filtering (ROKF) for HS reduction was proposed by (64). In this work, an autoregressive model was fitted to the HS segments free of respiratory sounds (i.e., breath hold segments including HS) under the adoption of three assumptions (i.e., heart and respiratory sounds are mutually uncorrelated; these sounds have additive interaction; and the prior and subsequent HS are linearly related to the HS corrupted by the respiratory signal). However, these prior assumptions make the method inefficient in practical implementations, and it was tested only with synthesized data and not actual LS; in addition, this ROKF-based approach exhibits increased computational cost.

Kompis and Russi (65) proposed a modification to the adaptive LMS algorithm (58), which combines the advantages of adaptive filtering with the convenience of using only a single microphone input, eliminating the need of recording a reference signal. Their modification consisted of adding a LPF with a cutoff frequency of 250 Hz in the error signal path to the filter. However, their results showed that HS were still clearly audible because of the improper identification of the HS segments within a long sound recording, achieving a moderate heart noise reduction by 24% up to 49%.

In the same perspective, yet with much better HS noise reduction results, another single recording adaptive noise cancellation (ANC) technique based on fourth-order statistics (FOS) was proposed by Hadjileontiadis and Panas (66). The ANC-FOS algorithm is an adaptive de-noising tool that employs a reference signal *z(k)* highly correlated with the HS noise. The ANC-FOS algorithm analyzes the incoming LS signal *x(k)* to generate the reference signal *z(k)*, by detecting the real location of the HS in the incoming LS signal. Therefore, the ANC-FOS scheme initially applies on $x(k)$ a peak detection algorithm, namely *localized reference estimation* (LOREE) algorithm (66), which searches for the true locations of HS noise, based on amplitude, distance, and noise-reduction percentage criteria. Its output, $z(k)$, is a localized signal with precise tracking of the first (S_1) and second (S_2) heartbeats, highly correlated with heart noise and with no extra recording requirement as Iyer's method requires (58). The basic characteristic of the ANC-FOS is that, during the adaptation procedure, its update equation consists only of the fourth-order cumulants of the incoming and reference signals, and it is not affected by Gaussian uncorrelated noise. This observation reveals the enhancement achieved in the robustness of an ANC scheme when FOS are employed in its structure. Comparing the ANC-FOS algorithm with the adaptive schemes proposed by Iyer et al. (58) and Kompis with Russi (65), it can be deduced that, unlike the latter, the ANC-FOS algorithm finds the true locations of S_1 and S_2 without assuming any similarity in the two HS. In addition, neither Iyer's nor Kompis' methods take into account any nonlinear transformation that might be necessary to correctly account for nonlinearities in the system, as the ANC-FOS algorithm does because of the employment of FOS. Furthermore, although Kompis' method, unlike Iyer's, avoids the need of extra recording, it results in moderate noise reduction percentages compared with that of the ANC-FOS scheme. Finally, both Iyer's and Kompis' methods are sensitive to additive Gaussian noise, whereas the ANC-FOS algorithm is insensitive to Gaussian uncorrelated noise and independent of it, because it is based on FOS, which are zero for Gaussian processes. An example of the output of the ANC-FOS, when applied on breath sound recordings contaminated with HS, is depicted in Fig. 2. From this figure, the efficiency of the ANC-FOS in deteriorating the HS noise leaving the LS signal unaffected is evident.

Recently, a bandpass-filtered version of the original signal was used as the reference input for an ANC-Recursive Least Squares (ANC-RLS) filtering technique (67). Although the performance of this method is promising

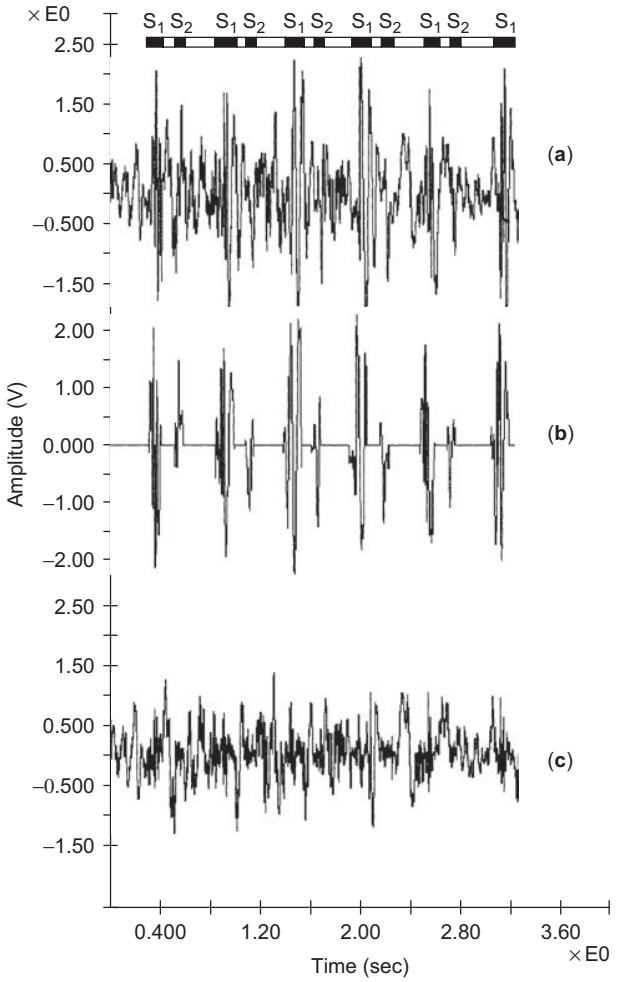

Figure 2. (a) Time waveform of 3.27-s raw contaminated LS recorded from a subject during normal breathing. (b) Time waveform of the corresponding reference signal [LOREE output (66)]. (c) Time waveform of adaptively filtered LS [ANC-FOS output (66)]. The small, black lines in the input tracing indicate the presence of the HS noise (S_1 and S_2 correspond to first and second HS, respectively).

both qualitatively and quantitatively, its computational load is quite high.

Multiresolution analysis, based on the discrete wavelet transform (WT), has also been used to form filtering techniques for the HS reduction from LS (68,69). In particular, in (69), an ANC-WT filter is proposed based on the fact that explosive peaks in the time-domain (HS peaks) have large signal amplitudes over many WT scales. On the contrary, "noisy" background (LS) dies out swiftly with increasing scale. The definition of "noise" is not always clear. For example, in this case, the HS peaks are temporary considered as the "desired" signal in order to be isolated from the LS (background noise); after their isolation, the residual (i.e., the de-noised LS) is now the desired signal and the isolated HS peaks are the noise. Hence, it is better to view an N-sample signal as being noisy or incoherent relative to a basis of waveforms if it does not correlate well with the waveforms of the basis (70). From this notion, the separation of HS from LS becomes a matter of breath sounds coherent structure extraction. The basic characteristic of the ANC-WT scheme is that, unlike most of the adaptive-filtering techniques, it does not need any reference signal for its adaptive performance. Comparing the ANC-WT algorithm (69) with the adaptive schemes proposed by Iyer et al. (59), Kompis and Russi (65), and the previously described ANC-FOS (66), it can be noticed that the ANC-WT scheme possesses all the advantages of the ANC-FOS algorithm over Iyer's and Kompis' methods, such as finding the true locations of S_1 and S_2 without assuming any similarity in the two HS, avoiding the need of extra recording, and resulting in high noise reduction. In addition, the ANC-WT scheme performs better than the ANC-FOS scheme when the additive noise has an impulsive character (e.g., friction sound caused by movement, impulsive ambient noise, etc). On the other hand, the ANC-FOS scheme performs better than the ANC-WT scheme when the input LS signal is contaminated by additive Gaussian uncorrelated noise (66,69). Although the ANC-WT algorithm results in smaller reduction percentages (84.1%) than the ANC-FOS algorithm ($>$ 90%), its "reference-free" structure equalizes this loss characterizing both of them as attractive noise reduction schemes. An example of the performance of the ANC-WT when applied on breath sound recordings contaminated with HS is depicted in Fig. 3. From this figure, the adaptation efficiency of the ANC-WT to HS noise reduction only is evident.

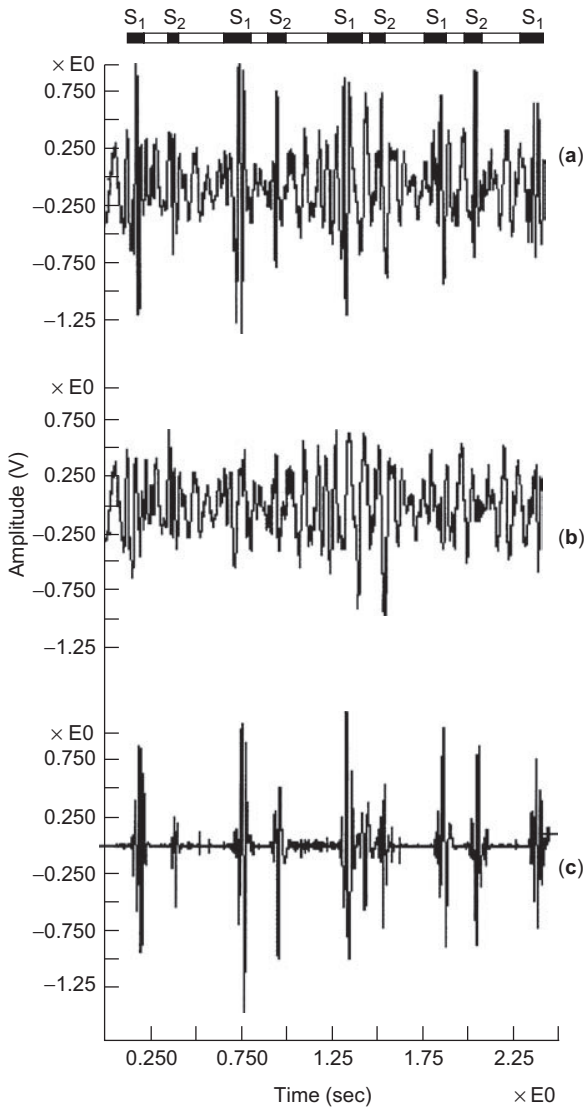

Figure 3. (a) Time waveform of 2.48-s raw contaminated LS recorded from a subject during normal breathing. (b) Time waveform of adaptively filtered LS [stationary ANC-WT output (69)]. (c) Time waveform of the estimated HS [nonstationary ANC-WT output (69)]. The small, black lines in the input tracing indicate the presence of the HS noise (S_1 and S_2 correspond to first and second HS, respectively).

4.1.2. Background Elimination-BAS Detection. The elimination of background noise in the BAS recordings is a major issue to be considered prior to their diagnostic analysis, because the presence of background noise severely influences the clinical auscultative interpretation of BAS. The elimination of noise results in de-noised BAS that provide a more reliable and accurate characterization of the associated pathology.

The noise sources in the case of the BS recordings include instrumentation noise introduced during the recording process, sounds from the stomach, as well as cardiac and respiratory sounds, which occur mostly in the case of infants. In order to yield a successful BS classification, an effective reduction of noise from the contaminated BS signal is required, because the presence of the noise introduces pseudoperiodicity, masks the relevant signal, and modifies the energy distribution in the spectrum of BS. From the available studies related to BS analysis, only a few are focused on the BS de-noising process in order to extract their original structure before any further diagnostic evaluation (30,71). Unfortunately, the method used for noise reduction in (30) was based only on assumptions and general descriptions of the noise characteristics, forming a static, rather than a dynamic, noise reduction scheme. In addition, the noise is manually extracted, after subjective characterization and localization of the noise presence in the histogram of the recorded BS. The

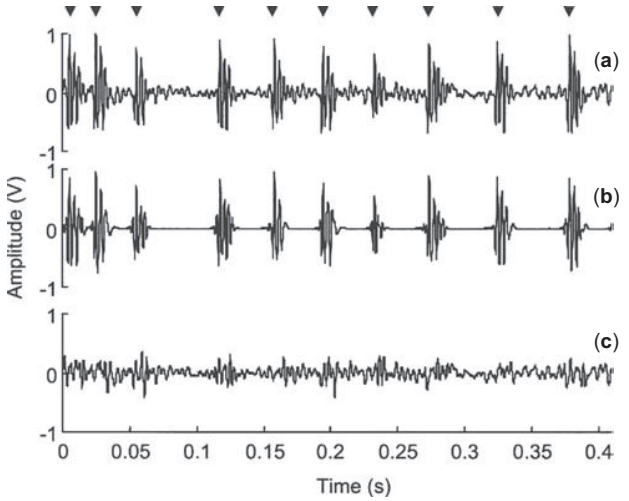

Figure 4. The performance of the ANC-WT filter when applied on recorded BS from a patient with irritable bowel syndrome (72). (a) The originally acquired BS signal. The arrowheads in the input tracing indicate the events of interest that correspond to BS. (b) The de-noised BS [nonstationary output of the ANC-WT filter (72)]. (c) The estimated background noise [stationary output of the ANC-WT filter (72)].

second de-noising method of BS, used by Mansy and Sandler (71), is based on adaptive filtering (60) and eliminates the HS noise from BS recorded from rats. Although it results in satisfactory enhancement of BS, it still requires careful construction of a noise reference signal, and it needs an empirical set-up of its adaptation parameters.

The previously described ANC-WT has been successfully applied to circumvent this problem (72). By a simple modification in its input (BS instead of LS), it results in efficient de-noising of BS signals, as it is apparent from Fig. 4.

Comparing the ANC-WT algorithm (72) with the adaptive scheme proposed by Mansy and Sandler (71), it can be noticed that, unlike the ANC-WT scheme, Mansy and Sandler's method is a "nonreference-free" scheme, because, apart from the BS recordings, it requires a reference signal for its performance. In addition, their scheme constructs a heart sound template, with averaged HS from previous successive heartbeats, to estimate the characteristics of the heart noise. On the contrary, it is not required by the ANC-WT scheme to describe the characteristics of the aggregated interference. Moreover, Mansy and Sandler's scheme is only tested on rats for the construction of the heart noise template, using their structural characteristics. On the contrary, the ANC-WT scheme is implemented in BS analysis derived from humans, with or without any gastrointestinal pathology. Finally, its implementation, unlike Mansy and Sandler's scheme, does not require empirical definition of a set of parameters, which is always prone to subjective human judgment.

As it was mentioned in the description of the LS characteristics in the LS section of this chapter, the DAS behave as a nonstationary explosive noise superimposed on breath sounds. The DAS are rarely normal, so their presence indicates an underlying pathological malfunction, which means that their separation from the background sound (i.e., the vesicular lung sounds or VLS) could reveal significant diagnostic information. In order to achieve automated separation, the nonstationarity of DAS must be taken into account. Thus, neither HP filtering, which destroys the waveforms, nor level slicing, which cannot overcome the small amplitude of FC, are adequate for this task. Application of time-expanded waveform analysis in crackle time-domain analysis (16,73) results in separation; it is, however, time-consuming, with large interobserver variability. Nonlinear processing, proposed by Ono et al. (74), and modified by Hadjileontiadis and Panas (75), obtains more accurate results, but requires empirical definition of the set of parameters of its *Stationary-nonstationary* (ST-NST) filter. To more efficiently overcome this problem (i.e., to achieve reliable automated separation of three types of DAS, namely fine crackles (or FC), coarse crackles (or CC), and squawks (or SQ), from VLS), a series of works have been proposed in the literature based on WT, fuzzy logic (FL), and fractal dimension (FD).

In particular, the WT-based method for automated separation of DAS from VLS refers to a form of the ANC-WT scheme adapted for this task. As the problem addressed here deals with the separation of the nonstationary part of the LS from the stationary part, the *ANC-WT scheme is renamed to wavelet transform-based ST-NST* (WTST-NST) filter, originally introduced by Hadjileontiadis and Panas (76). The only changes needed to the ANC-WT scheme refer to the input signal, which is now the breath sounds (DAS and VLS), and to the two outputs (nonstationary and stationary) corresponding to the separated DAS and the background VLS, respectively. Comparing the results of the WTST-NST algorithm (76) with those derived from the application of the nonlinear scheme (ST-NST) proposed by Ono et al. (74) at the same breath sounds [analytically shown in Table II in (76)], it is clear that the WTST-NST filter performs better than the ST-NST filter in all cases of each type of DAS, which is a result of the empirical definition of the parameters employed in the performance of the ST-NST filter, depending on the characteristics of the input signal. The WTST-NST filter may be applied to all types of DAS requiring neither empirical definition nor adaptive updating of its parameters according to the characteristics of the input signal. In addition, the WTST-NST filter, unlike the ST-NST filter, separates the whole DAS, without leaving the later parts (i.e., the part of DAS that follows the initial peak). Regarding the performance of the WTST-NST filter with that of the rest of separation techniques mentioned before, the WTST-NST filter clearly overcomes the disadvantages of HP filtering, because it results in nondestroyed DAS and VLS; unlike a level slicer it detects all DAS, even those with small amplitude, and unlike time-expanded waveform analysis (16,73), it results in accurate, fast, and objective results, regardless of DAS type and without employing any human intervention.

Although the WTST-NST filter obtains the most accurate separation results among all other methods reported in the recent literature, it cannot serve as the optimum solution when the real-time analysis of the LS is the primary aim. To this end, enhanced *real-time* DAS detectors

based on FL have been proposed. The first one, namely *generalized FST-NST* (GFS-NST) filter, is based on a generalized version of the *fuzzy logic-based ST-NST* (FST-NST) filter proposed by Tolias et al. (77), and uses one *fuzzy inference system* (FIS) dedicated to the estimation of the stationary part of the signal to provide a reference to the second FIS that estimates the nonstationary part (78). In an alternative approach in developing fuzzy models for real-time separation of DAS from VLS, the model generation process is based on the *Orthogonal Least Squares* (OLS) concept (79), providing structure and parameter identification, as well as performing input selection. In particular, the parameters of the resulting models are calculated in a forward manner without requiring an iterative training algorithm. Therefore, the method does not suffer from drawbacks inherent to gradient-based techniques, such as tapping to local minima and extensive training time. This approach uses two FISs that operate in parallel and form the *OLS-based fuzzy filter* (OLS-FF) (80). In general, the OLS-FF improves the structure employed in (78), introducing a more flexible architecture. As a result, it activates the optimum employed fuzzy rules, uses a lower number of rules, and comprises the most appropriate inputs for each of them, which is a clear advantage over the previous work (78), because the latter uses a complete rule base and consequent parts with fixed number of terms. In addition, unlike the GFST-NST filter, the OLS-FF does not require a training phase for the estimation of the optimum model parameters, because they are calculated on the spot. Although the OLS-FF exhibits an inferior performance compared with the WTST-NST filter (76), it satisfies the real-time implementation issue. However, the GFST-NST filter (78) performs better than the OLS-FE by 1% up to 4% for the cases of CC and SQ, and by 14% for the case of FC as a trade-off between the structural simplicity of the OLS-FF. On the contrary, the OLS-FF requires a significantly smaller (by 62%) computational load than the GFST-NST filter, improving the procedure of clinical screening of DAS under a real-time implementation context (80,81). Figure 5 illustrates

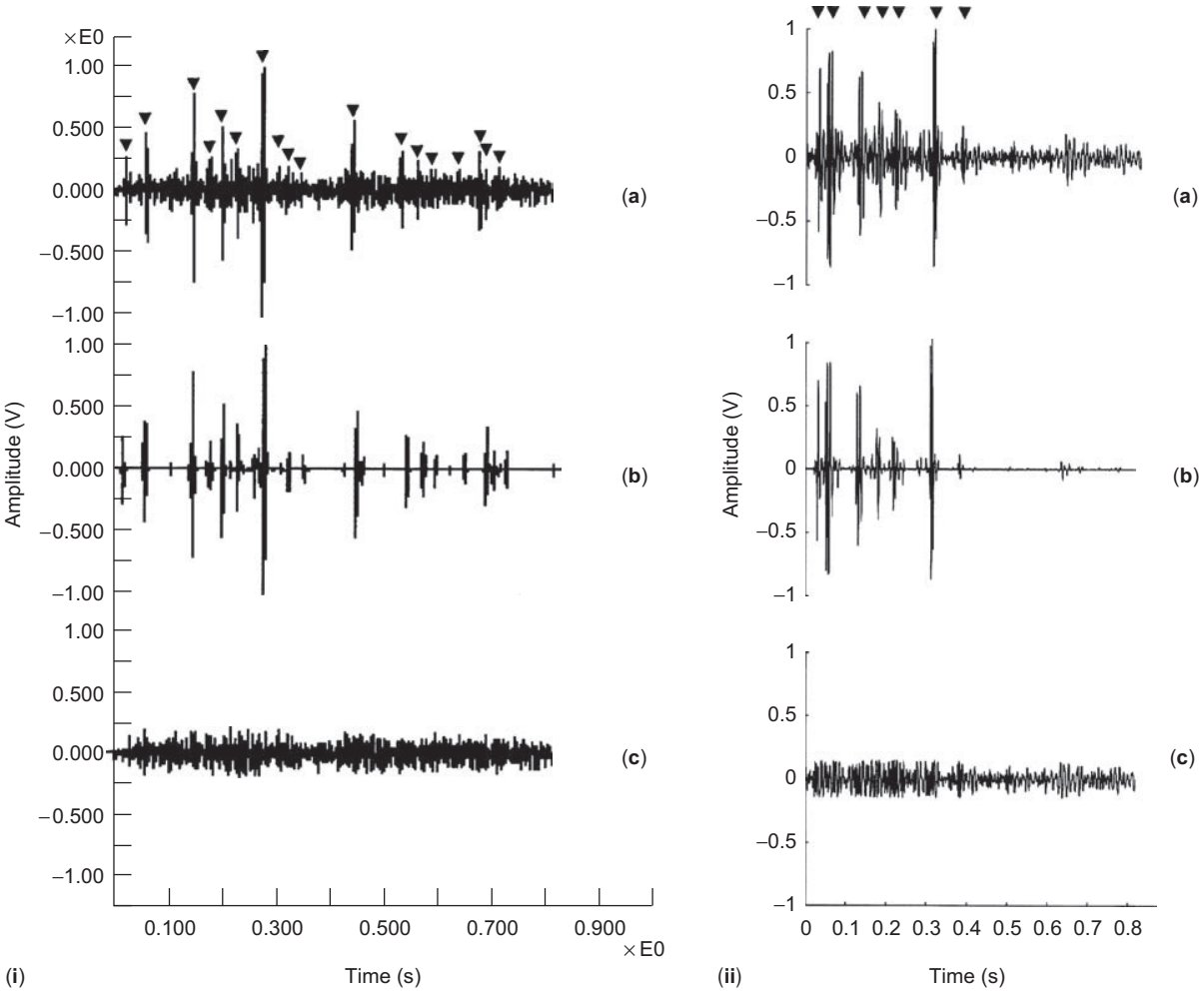

Figure 5. Examples from the performance of (i) the WTST-NST filter (76) on FC and (ii) the GFST-NST filter (78) on CC. In both subfigures, (a)–(c) correspond to the input signal, the estimated denoised BAS, and the estimated background noise, respectively. Furthermore, the arrowheads in both input tracings indicate the events of interest that correspond to BAS.

some examples of the performance of the WTST-NST and the GFST-NST filters.

Recently, an FD-based approach has been proposed to address the detection of DAS in the LS signal and of BS in the background noise (82). In particular, this technique forms an FD-based detector (FDD), which assesses the complexity of the sound recordings in the time-domain in order to efficiently detect the time location and duration of the nonstationary LS and BS. As nonstationarity is the key feature for the detection of these sound recordings, its direct relationship with the signal complexity makes the FD measure a possible tool for their detection. Compared with the previous approaches (75–78,80,83), the FDD is more attractive because of the simplicity in the evaluation of the FD measure, because the FDD is a time-domain FD algorithm that operates directly on the signal and not on state space, and hence it has fast computational implementation.

4.1.3. Reduction of Interference in TMJS and HS Time-Frequency Representation. Time-frequency signal analysis has recently experienced an accelerating development of interest. Although spectrogram and Wigner–Ville distribution [both members of Cohen's Class of Distributions (84)] have been used in tracking the frequency content of nonstationary signals, they both exhibit liabilities, such as failure to resolve signal components close in frequency and production of interference (cross terms) because of interactions between signal components, respectively. To this end, Williams and Jeong have proposed a *reduced interference distribution* (RID) (85,86), aiming at achieving high-resolution time-frequency distributions within Cohen's class with much reduced cross-term or interference activity. The suppression of cross terms was achieved by attenuating distant terms in the ambiguity-domain, at the same time retaining a number of other desirable mathematical properties, which are not exhibited by other members of Cohen's class (85,86). The RID-based analysis of TMJS (50,86–88) provided the successful categorization of TMJS to five types described in the Joint Sounds section of this chapter.

In a similar vein, Wood and Barry and their colleagues (89–92) used the binomical form of the RID in the HS analysis in order to clearly track the alterations of the dynamic changes in physiological properties caused by pathology. Guo et al. (93,94) devised the Bessel kernel that generally falls into the RID class, exhibiting further advantages in the HS analysis, particularly of valve sounds. They have also found that, by increasing the computational burden and relaxing some of the constraints on the distribution, like the time support constraint such that the kernel is integrating (or summing) over a larger range of signal values, the noise is further suppressed (93,94).

4.2. Modeling

Modeling of the system that produces the BAS contributes to the understanding of their production mechanisms. The way the pathology affects these mechanisms is reflected in the modeling parameters adopted, which is a very important issue in the analysis of BAS, because efficient modeling could lead to an objective description of the changes a disease imposes to the production or transmission path of the BAS.

LS originated inside the airways of the lung are modeled as the input to an all-pole filter, which describes the transmission of LS through the parenchyma and chest wall structure (95). The output of this filter is considered to be the LS recorded at the chest wall. As it is already mentioned in previous subsections, the recorded LS also contain heart sound interference, the reduction of which has been thoroughly addressed in the Noise Reduction-Detection section of this chapter. Muscle and skin noise, along with instrumentation noise, are modeled as an additive Gaussian noise. With this model, given a signal sequence of LS at the chest wall, an *autoregressive* (AR) analysis based on *third-order statistics* (TOS), namely AR-TOS, can be applied to compute the model parameters. Therefore, the source and transmission filter characteristics can be separately estimated, as it is thoroughly described in (81,96). The profound motivations behind the use of the AR-TOS model is the suppression of Gaussian noise, because TOS of Gaussian signals are identically zero. Hence, when the analyzed waveform consists of a nonGaussian signal in additive symmetric noise (e.g., Gaussian), the parameter estimation of the original signal with TOS takes place in a high-SNR domain, and the whole parametric presentation of the process is more accurate and reliable (97,98). The model used for the LS originated inside the airways considers the LS source as the output from an additive combination of three kinds of noise sequences (14). The first sequence (periodic impulse) describes the *CAS sources*, because they have characteristic distinct pitches, and they are produced by periodic oscillations of the air and airway walls (see also the Categorization and Main Characteristics subsection of Lung Sounds) (9,17). The second sequence (random intermittent impulses) describes the *crackle sources*, because they are produced by sudden opening/closing of airways or bubbling of air through extraneous liquids in the airways, both phenomena associated with sudden intermittent bursts of sounds energy (see also the Categorization and Main Characteristics subsection of Lung Sounds) (9,17). Finally, the third sequence (white nonGaussian noise) describes the *breath sound sources*, because they are produced by turbulent flow in a large range of airway dimensions (see also the Categorization and Main Characteristics subsection of Lung Sounds) (9,17). The estimation of the AR-TOS model input (LS source) can be derived from the prediction error by means of inverse filtering (96,99).

As it was described in the Lung Sounds section, among the different kinds of BAS recorded from the human body, some exhibit sharp peaks or occasional bursts of outlying observations that one would expect from normally distributed signals, such as the DAS and some types of impulsive BS. In addition, these BAS occur with a different *degree* of impulsiveness. As a result of their inherent impulsiveness, these BAS have a density function that decays in the tails less rapidly than the Gaussian density function (100). Modeling based on *alpha-stable distribution* is appropriate for enhanced description of impulsive processes (100).

Furthermore, under the nonGaussian assumption in the context of analyzing impulsive processes, among the various distribution models that were suggested in the past, the *alpha*-stable distribution is the only one that is motivated by the *generalized central limit theorem*. This theorem states that *the limit distribution of the sum of random variables with possibly infinite variances is stable distribution* (101). Stable distributions are defined by the stability property, which says that *a random variable, X, is stable if and only if the sum of any two independent random variables with the same distribution as X also has the same distribution* (101). Following this approach, impulsive LS (i.e., DAS) and BS with explosive character can be modeled by means *of alpha-stable distribution, symmetrical alpha-stable* ($S\alpha S$) distribution, and *lower-order statistics* (LOS) (102). From the estimated parameters of the ($S\alpha S$) distribution of the analyzed impulsive BAS with the $\log|S\alpha S|$ method (100) (because the fractile method (103) works only for $\alpha \geq 0.6$, and the regression method (104), needs empirical parameter setting), it is derived that when the contaminated (without de-noising) impulsive BS are analyzed, the values of α are large enough (near 1.5), whereas when the AR-estimated inputs of the de-noised data are analyzed, these values decrease dramatically. This fact is because of the increase of impulsiveness of the analyzed signal, since the vesicular sound and the background noise are suppressed after de-noising. In fact, the impulsive source sound, initiated inside the lung or the bowel, reaches the surface with different signal characteristics, indicating a shifting toward the Gaussian distribution because of the superimposed Gaussian noise. Generally, the values of dispersion γ are low enough, indicating small deviation around the mean, whereas the location parameter a has mean values around zero, indicating low mean and median for $1<\alpha \leq 2$ and $0<\alpha<1$, respectively (102). The *covariation coefficient* λ_{SQ-FC} calculated for the cases of the sound sources of SQ and FC (102) shows an almost 50% correlation between the SQ and FC, confirming the accepted theory that SQ are produced by the explosive opening, because of a FC, and decaying fluttering of an unstable airway (9,17), which proves that $S\alpha S$ distribution- and LOS-based modeling of impulsive BAS provide a measure of their impulsiveness, and, at the same time, reveals the underlying relationships between the associated production mechanisms and pathology.

4.3. Feature Extraction Classification

The characteristics of BAS provide a variety of structural features that are directly connected to the underlined pathology. The correlation of these features with parameters derived from advanced processing of BAS provides a means for their efficient classification and, consequently, for the classification of the associated pathology.

The LS that are characterized as musical are the CAS [i.e., wheezes (WZ), rhonchi (RH), and stridors (STR)] described the Categorization and Main Characteristics subsection of Lung Sounds. The musical character of these LS is reflected to the power spectrum through distinct frequency peaks (14). As the second-order statistics suppress any phase information, they fail to detect and characterize the nonlinear interactions of the distinct harmonics. Spectral-based methodologies have been widely applied to frequency-domain analysis of musical LS (mainly wheezes) (14,105,106). They, however, do not take into account the nonlinearity and nonGaussianity of the analyzed processes. On the contrary, *higher-order statistics* (HOS) preserve the phase character of the signals (97) and have been used as a useful tool for the detection of nonlinearity and deviation from Gaussianity of the signals. In this way, the process of musical LS is expanded to more accurate estimations of their true character. In particular, based on the results presented in (107), it can be concluded that a strong quadratic phase coupling exists among the distinct harmonics of the musical HS along with a strong nonGaussianity of the analyzed processes for the case of increased pathology.

Furthermore, bispectral analysis of HS (108) indicate that more efficient discrimination of cardiac pathologies could be established in the bispectrum-domain [higher (>2)-order spectrum] rather in the power spectrum one, which can be used for further elicitation of the diagnostic character of HS.

Moreover, bispectral analysis of BS (109) shows the ability of bispectrum to differentiate the BS recorded from a patient with bowel polyp before and after the polypectomy, hence to reflect the anatomical changes of the bowel. In addition, in (109), HOS-based analysis of BS recorded from controls shows a strong deviation from normality and linearity; for BS recorded from patients with diverticular disease, it shows increased nonGaussianity and decreased nonlinearity; for BS recorded from patients with ulcerative colitis, it reveals a strong deviation from normality and linearity; and for BS recorded from patients with irritable bowel syndrome, it results in increased nonGaussianity and decreased nonlinearity (109). These results show that HOS provide a new perspective in the computerized analysis of BS, defining an enhanced field of new features, which reinforce the diagnostic character of BS.

Considering the nonGaussianity and the impulsiveness of crackles and artifacts, we could model them as $S\alpha S$-distributed processes, in the way it is described in the Modeling section of this chapter. By estimating the characteristic exponent α for each category (crackles, background noise, and artifacts) using the $\log|S\alpha S|$ method (100), a classification criterion could be established based on the estimated *alpha* values. This approach has been adopted in (110), which deduces that the FC follow approximately the Cauchy distribution (mean $\alpha = 0.92$, which is close to $\alpha = 1.0$ and holds in the case of the Cauchy distribution), whereas the CC deviate both from Cauchy and Gaussian distributions (mean $\alpha = 1.33$). The artifacts have high impulsiveness (mean $\alpha = 0.0218$). The events that resemble the vesicular sound are seen as background noise and are modeled as Gaussian processes (values of $\alpha > 1.8$ or very close to 2.0; a value that holds in the case of the Gaussian distribution).

Higher-order crossings (HOC) [i.e., the zero-crossing counts resulting from the application of a bank of filters to a time series (111)] have also been applied in the classification analysis of BAS, because HOC constitute a domain

by itself, which "sits" between the time- and spectral-domains (111). Consequently, the use of the *white noise test* (WNT) (i.e., the measurement of the distance of the signals under consideration from white Gaussian noise) and the *HOC-scatter plot* (HOC-SP), which is a scattergram that depicts a pair of simple HOC (D_j, D_k) (111), can be used for the BAS classification. In particular, the WNT is employed so the two categories of the signals, for example, FC and CC, are indirectly compared with each other. The ith order of HOC that results in the maximum distance between the two categories, defined as the maximum distance from the lower curve of one category to the upper curve of the other at the ith order, provides with a linear discrimination in the HOC domain. In particular, by plotting D_i versus $D_{i\pm m}$, where m usually equals 1, 2, or 3 (for $i \geq 5$), the resulted HOC-SP reveals two *linearly* separated classes. As a result of the linear character of the separation, a simple single-layer perceptron neural network (112) can be used for decision on class membership.

Results from the HOC-based analysis of crackles (113), initially de-noised with the WTST-NST filter (76), are illustrated in Fig. 6. From Fig. 6a, it is clear that the order, which provides with the maximum distance between FC and CC, the so-called "opened-eye," equals 12 (denoted by an arrow). This distance is reflected to the corresponding HOC-SP (D_{12}, D_{13}) of Fig. 6b, where FC and CC are concentrated in two distant, linearly separated classes. These results indicate that the HOC-based indices result in fast, easy, and efficient discrimination of crackles, providing with a simple decision rule for categorizing FC and CC.

Further application of HOC-based classification of BAS includes discrimination between normal LS and abnormal bronchial LS heard over the trachea (tracheobronchial LS) (114); de-noised BS recorded from patients with different pathologies of the large bowel, such as ulcerative colitis and diverticular disease; and de-noised BS recorded from patients with small volume ascites and controls (115). In all referenced cases, a linear separation is feasible, exhibiting the potentiality of the HOC-based analysis to provide an efficient classification domain in a diversity of BAS types.

Classification of TMJS from joint with and without effusion using spectrogram-based analysis is presented in (116) where it is concluded that joints with effusion can be identified through the unstable sound patterns as they are revealed in the time-frequency domain. In this way, screening of patients with suspected effusion is much more simple and less expensive than the current use of magnetic resonance imaging.

The way the head tissues affect spectral characteristics of TMJS and how these differences (because of different positioning of sensors) can be used in the localization of source are explored in (117). They conclude that spectral analysis of bilateral electronic TMJS recordings is of diagnostic value when bilateral clicking is heard at auscultation and can help to avoid diagnosing a silent joint as clicking.

Wavelet transform-based representations of TMJS are used in (118) to visually differentiate between controls and patients with reducing displaced disks. A 3×7 biorthogonal spline WT is used to create three-dimensional time-frequency graphs of the TMJS from each category, resulting in distinct visual differences between patients and controls (118).

In parallel to the aforementioned approaches, a number of research efforts have been placed on the computerized classification of TMJS, especially in the RID-analysis domain. In particular, replacement of the visual analysis

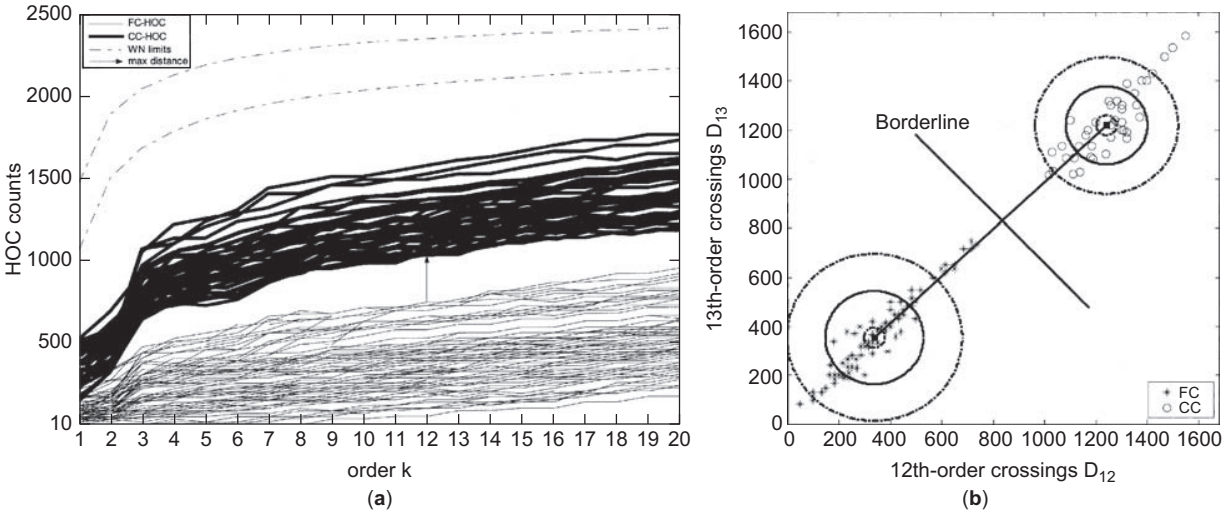

Figure 6. (a) Results from the WNT for FC and CC with the HOC order ranging from 1 to 20. The estimated HOC sequences of FC (FC-HOC) and CC (CC-HOC) are compared with the white noise (WN) limits. The maximum distance between FC-HOC (most upper) and CC-HOC (most lower) lines is denoted with an arrow located at the 12th HOC order. (b) Scatter plot of 12th-order (D_{12}) vs. 13th-order (D_{13}) crossings of FC (stars) and CC (circles). The ■ symbol denotes the center of each group (FC and CC), whereas borderline is the estimated linear border that clearly discriminates the two groups. The solid and dash-dotted circles correspond to [mean value ± (standard deviation + standard error of the mean)] of the distance from cluster center, both for FC and for CC.

of RIDs of the TMJS (an expensive and error-prone procedure) with neural networks has been proposed in (119). Adaptive Gabor transforms (120) and the third-order Rényi number of the RIDs were also used for discrimination among the five TMJS types (see the Joint Sounds section of this chapter), especially for the differentiation between the clickings and the crepitations (120). Yang et al. (121) used neural networks-, nearest linear combination-, and nearest constrained linear combination-based classifiers to automatically distinguish between types 1–3 of the TMJS classes (see the Joint Sounds section of this chapter). Finally, an extension of Yang's work, employing concepts of time-shift invariance with and without scale in variance, is presented in (122), which shows that the classifier performance is significantly improved when scale invariance is omitted.

Spectrogram-based analysis of KJS from patients with end-stage osteoarthritis, patellofemoral joint disorders, and lateral meniscal bucket handle tears is presented in (123). They have found a distinct shift of the spectrum to lower frequencies after intra-articular injection of Hyaluronic acid to the knee, establishing an efficient way of measuring the improvement of the lubricative functions through the spectral characteristics of KJS.

The use of matching pursuit method (124) in creating high-resolution and interference-free time-frequency representations of KJS is presented in (125). They involve time-frequency features, such as instantaneous energy, instantaneous energy spread, instantaneous frequency, and instantaneous frequency spread, in order to classify KJS from normal and abnormal knees. They report classification accuracy up to 86%, exhibiting high sensitivity in screening patellofemoral articular cartilage disorders, such as chondromalacia patella. Furthermore, they employ Hough (126) and Radon (127) transforms in order to extract patterns/signatures from the time-frequency domain, which could aid in better screening and understanding of how the movement of knee affects KJS patterns.

The issues presented here adopt the same endeavor: exploitation and surfacing of the valuable diagnostic information that exists in bioacoustic signals. Under this common aim, the different approaches of de-noising, detection, modeling, feature extraction, and classification described here introduce new pathways in the analysis of BAS, toward a noninvasive, efficient, and objective evaluation and understanding of the human body functioning.

BIBLIOGRAPHY

1. Houghton Mifflin Company (2000). *The American Heritage Dictionary of the English Language*, 4th ed. (online). Available: *http://www.dictionary.com/cgi-bin/dict.pl?term=bioacoustics.*
2. V. S. McKusick, *Cardiovascular Sound in Health and Disease.* Baltimore, MD: Williams & Wilkins, 1958, p. 3.
3. J. Rapoport, Laënnec and the discovery of auscultation. *Israel J. Med*. 1986; **22**:597–601.
4. V. S. McKusick, *Cardiovascular Sound in Health and Disease.* Baltimore, MD: Williams & Wilkins, 1958, p. 13.
5. S. S. Kraman, Vesicular (normal) lung sounds: how are they made, where do they come from and what do they mean? *Semin. Respir. Med*. 1985; **6**:183–191.
6. R. E. Thacker and S. S. Kraman, The prevalence of auscultatory crackles in subjects without lung disease. *Chest* 1982; **81**(6):672–674.
7. P. Workum, S. K. Holford, E. A. Delbono, and R. L. H. Murphy, The prevalence and character of crackles (rales) in young women without significant lung disease. *Amer. Rev. Respir. Dis.* 1982; **126**(5):921–923.
8. A. J. Robertson, Rales, ronchi, and Laënnec. *Lancet* 1957; **1**:417–423.
9. S. S. Kraman, *Lung Sounds: An Introduction to the Interpretation of Auscultatory Findings.* Northbrook, IL: American College of Chest Physicians, 1983, pp. 14–21.
10. R. L. H. Murphy, Discontinuous adventitious lung sounds. *Semin. Respir. Med*. 1985; **6**:210–219.
11. D. W. Cugell, Lung sound nomenclature. *Am. Rev. Respir. Dis.* 1987; **136**:1016.
12. J. E. Earis, K. Marsh, M. G. Rearson, and C. M. Ogilvie, The inspiratory squawk in extrinsic allergic alveolitis and other pulmonary fibroses. *Thorax* 1982; **37**(12):923–936.
13. N. Gavriely and D. W. Cugell, *Breath Sounds Methodology.* Boca Raton, FL: CRC Press, 1994, p. 2.
14. N. Gavriely, Y. Palti, and G. Alroy, Spectral characteristics of normal breath sounds. *J. Appl. Physiol.* 1981; **50**:307–314.
15. T. Katila, P. Piirila, K. Kallio, E. Paajanen, T. Rosqvist, and A. R. A. Sovijarvi, Original waveform of lung sound crackles: a case study of the effect of high-pass filtration. *J. Appl. Physiol.* 1991; **71**(6):2173–2177.
16. R. L. H. Murphy, S. K. Holford, and W. C. Knowler, Visual lung-sound characterization by time-expanded wave-form analysis. *New Eng. J. Med*. 1978; **296**:968–971.
17. N. Gavriely and D. W. Cugell, *Breath Sounds Methodology.* Boca Raton, FL: CRC Press, 1994, p. 8.
18. B. Erickson, *Heart Sounds and Murmurs: A Practical Guide,* 3rd ed. St. Louis, MD: Mosby-Year Book, 1997, p. 2.
19. R. C. Cabot and H. F. Dodge, Frequency characteristics of heart and lung sounds. *JAMA* 1925; **84**:1793–1795.
20. N. Gavriely and D. W. Cugell, *Breath Sounds Methodology.* Boca Raton, FL: CRC Press, 1994, p. 116.
21. A. P. Yoganathan, R. Gupta, J. W. Miller, F. E. Udwardia, W. H. Corcoran, R. Sarma, J. L. Johnson, and R. J. Bing, Use of the fast Fourier transform for frequency analysis of the first heart sound in normal man. *Med. Biol. Eng*. 1976; **1**:69–81.
22. Academic Medical Publishing & Cancer WEB. (1997). *Online Medical Dictionary* (online). Available: *http://www.graylab.ac.uk/cgi-bin/omd?bowel+sounds*.
23. W. B. Cannon, Auscultation of the rhythmic sounds produced by the stomach and intestine. *Am. J. Physiol*. 1905; **13**:339–353.
24. G. E. Horn and J. M. Mynors, Recording the bowel sounds. *Med. Biol. Eng.* 1966; **4**:205–208.
25. W. C. Watson and E. C. Knox, Phonoenterography: the recording and analysis of BS. *Gut*. 1967; **8**:88–94.
26. D. Dalle, G. Devroede, R. Thibault, and J. Perrault, Computer analysis of BS. *Comp. Biol. Med*. 1975; **4**:247–256.
27. J. P. Politzer, G. Devroede, C. Vasseur, J. Gerand, and R. Thibault, The genesis of bowels sounds: influence of viscus and gastrointestinal content. *Gastroenterology* 1976; **71**:282–285.
28. J. Weidringer, S. Sonmoggy, B. Landauer, W. Zander, F. Lehner, and G. Blumel, BS recording for gastrointestinal

motility. In: M. Weinbeck, ed., *Motility of the Digestive Track*. New York: Raven Press, 1982, pp. 273–278.

29. S. Michael and M. Redfern, Computerized Phonoenterography: the clinical investigation of a new system. *J. Clin. Gastroenterol*. 1994; **18**(2):139–144.
30. H. Yoshino, Y. Abe, T. Yoshino, and K. Ohsato, Clinical application of spectral analysis of BS in intestinal obstruction. *Dis. Col. Rect*. 1990; **33**(9):753–757.
31. R. H. Sandler, H. A. Mansy, S. Kumar, P. Pandya, and N. Reddy, Computerized analysis of bowel sounds in human subjects with mechanical bowel obstruction vs. ileus. *Gastroenterology* 1993; **110**(4):A752.
32. D. Bray, R. B. Reilly, L. Haskin, and B. McCormack, Assessing motility through abdominal sound monitoring. In: B. Myklebust and J. Myklebust, eds., Proc. 19th Annu. Int. Conf. IEEE/EMBS, Chicago, IL: IEEE Press, 1997, pp. 2398–2400.
33. B. L. Craine, M. L. Silpa, and C. J. O'Toole, Enterotachogram analysis to distinguish irritable bowel syndrome from Crohn's disease. *Dig. Dis. Sci.* 2001; **46**(9):1974–1979.
34. M. S. Spiller, (2000) TMJ (online). Available: *http://www.doctorspiller.com/TMJ.htm*.
35. C. Heuter, *Grundiss der Chirurfie,* 3rd ed. Leipzig, Germany: FCW Vogel, 1885.
36. W. E. Blodgett, Auscultation of the knee joint. *Boston Med. Surg. J.* 1902; **146**(3):63–66.
37. E. Bircher, Zur diagnose der meniscusluxation und des meniscusabrisses. *Zentralbl. Chir.* 1913; **40**:1852–1857.
38. C. F. Walters, The value of joint auscultation. *Lance*t 1929; **1**:920–921.
39. K. H. Erb, Uber die moglichkeit der registrierung von gelenkgerauschen. *Deutsche Ztschr. Chir.* 1933; **241**:237–245.
40. A. Steindler, Auscultation of joints. *J. Bone Int. Surg.* 1937; **19**:121–124.
41. A. Peylan, Direct auscultation of the joints (Preliminary clinical observations). *Rheumatism* 1953; **9**:77–81.
42. H. Fischer and E. W. Johnson, Analysis of sounds from normal and pathologic knee joints. Proc. 3rd Int. Congr. Phys. Med., 1960: 50–57.
43. M. L. Chu, I. A. Gradisar, M. R. Railey, and G. F. Bowling, Detection of knee joint diseases using acoustical pattern recognition technique. *J. Biomechan*. 1976; **9**:111–114.
44. M. L. Chu, I. A. Gradisar, and R. Mostardi, A non-invasive electroacoustical evaluation technique of cartilage damage in pathological knee joints. *Med. Biologic. Engineer. Comput*. 1978; **16**:437–442.
45. R. A. B. Mollan, G. C. McCullagh, and R. I. Wilson, A critical appraisal of auscultation of human joints. *Clin. Orthopaed. Related Res.* 1982; **170**:231–237.
46. W. G. Kernohan and R. A. B. Mollan, Microcomputer analysis of joint vibration. *J. Microcomp. Applicat*. 1982; **5**:287–296.
47. R. A. B. Mollan, W. G. Kernohan, and P. H. Watters, Artefact encountered by the vibration detection system. *J. Beomechan*. 1983; **16**(3):193–199.
48. W. G. Kernohan, D. E. Beverland, G. F. McCoy, S. N. Shaw, R. G. H. Wallace, G. C. McCullagh, and R. A. B. Mollan, The diagnostic potential of vibration arthrography. *Clinic. Orthopaed. Related Res.* 1986; **210**:106–112.
49. G. F. McCoy, J. D. McCrea, D. E. Beverland, W. G. Kernohan, and R. A. B. Mollan, Vibration arthrography as a diagnostic aid in diseases of the knee. *J. Bone Joint Surg.* 1987; **B**(2):288–293.
50. S. E. Widmalm, W. J. Williams, R. L. Christiansen, S. M. Gunn, and D. K. Park, Classification of temporomandibular joint sounds based upon their reduced interference distribution. *J. Oral Rehab.* 1996; **23**:35–43.
51. C. B. Frank, R. M. Rangayyan, and G. D. Bell, Analysis of knee joint sound signals for non-invasive diagnosis of cartilage pathology. *IEEE Eng. Med. Biol. Mag.* 1990; **9**(1):65–68.
52. L. Vannuccini, J. E. Earis, P. Helistö, B. M. G. Cheetham, M. Rossi, A. R. A. Sovijärvi, and J. Vanderschoot, Capturing and preprocessing of respiratory sounds. *Eur. Respir. Rev.* 2000;**10**(77):616–620.
53. M. J. Mussell, The need for standards in recording and analysing respiratory sounds. *Med. Biol. Eng. Comput*. 1992; **30**:129–139.
54. S. E. Widmalm, W. J. Williams, and B. S. Adams, The wave forms of temporomandibular joint sounds clicking and crepitation. *J. Oral Rehab.* 1996; **23**:44–49.
55. V. K. Iyer, P. A. Ramamoorthy, and Y. Ploysongsang, Quantification of heart sounds interference with lung sounds. *J. Biomed. Eng.* 1989; **11**:164–165.
56. N. J. McLellan and T. G. Barnett, Cardiorespiratory monitoring in infancy with acoustic detector. *Lancet* 1983; **2**(8364):1397–1398.
57. A. Tal, I. Sanchez, and H. Pasterkamp, Respisonography in infants with acute bronchiolitis. *Am. J. Dis. Child*. 1991; **145**:1405–1410.
58. V. K. Iyer, P. A. Ramamoorthy, H. Fan, and Y. Ploysongsang, Reduction of heart sounds from lung sounds by adaptive filtering. *IEEE Trans. Biomed. Eng*. 1986; **33**(12):1141–1148.
59. Y. Ploysongsang, V. K. Iyer, and P. A. Ramamoorthy, Characteristics of normal lung sounds after adaptive filtering. *Am. Rev. Respir. Dis*. 1989; **139**:951–956.
60. B. Widrow, J. R. Glover, J. McCool, M. J. Kaunitz, C. S. Williams, R. H. Hearn, J. R. Zeidler, E. Dong, and R. C. Goodlin, Adaptive noise canceling: principles and applications. *Proc. IEEE* 1975; **63**(12):1692–1716.
61. L. Yang-Sheng, L. Wen-Hui, and Q. Guang-Xia, Removal of the heart sound noise from the breath sound. Proc. 10th Annu. Int. Conf. IEEE/EMBS 1988: 175–176.
62. L. Guangbin, C. Shaoqin, Z. Jingming, C. Jinzhi, and W. Shengju, The development of a portable breath sounds analysis system. Proc. 14th Annu. Int. Conf. IEEE/EMBS 1992: 2582–2583.
63. L. Yip and Y. T. Zhang, Reduction of heart sounds from lung sound recordings by automated gain control and adaptive filtering techniques. Proc. 23rd Annu. Int. Conf. IEEE/EMBS 2001: 2154–2156.
64. S. Charleston and M. R. Azimi-Sadjadi, Reduced order Kalman filtering for the enhancement of respiratory sounds. *IEEE Trans. Biomed. Eng.* 1996; **43**(4):421–424.
65. M. Kompis and E. Russi, Adaptive heart-noise reduction of lung sounds recorded by a single microphone. Proc. 14th Annu. Int. Conf. IEEE/EMBS 1992: 691–692.
66. L. J. Hadjileontiadis and S. M. Panas, Adaptive reduction of heart sounds from lung sounds using fourth-order statistics. *IEEE Trans. Biomed. Eng.* 1997; **44**(7):642–648.
67. J. Gnitecki, Z. Moussavi, and H. Pasterkamp, Recursive least squares adaptive noise cancellation filtering for heart sound reduction in lung sounds recordings. Proc. 25th Annu. Int. Conf. IEEE/EMBS 2003: 2416–2419.
68. I. Hossain and Z. Moussavi, An overview of heart-noise reduction of lung sound using wavelet transform based filter. Proc. 25th Annu. Int. Conf. IEEE/EMBS 2003: 458–461.

69. L. J. Hadjileontiadis and S. M. Panas, A wavelet-based reduction of heart sound noise from lung sounds. *Int. J. Med. Infor.* 1998; **52**:183–190.

70. R. Coifman and M. V. Wickerhauser, Adapted waveform 'denoising' for medical signals and images. *IEEE Eng. Med. Biol. Soc.* 1995; **14**(5):578–586.

71. H. A. Mansy and R. H. Sandler, Bowel-sound signal enhancement using adaptive filtering. *IEEE Eng. Med. Biol.* 1997; **16**(6):105–117.

72. L. J. Hadjileontiadis, C. N. Liatsos, C. C. Mavrogiannis, T. A. Rokkas, and S. M. Panas, Enhancement of bowel sounds by wavelet-based filtering. *IEEE Trans. Biomed. Eng.* 2000; **47**(7):876–886.

73. R. Loudon and R. L. Murphy, Jr., Lung sounds. *Amer. Rev. Respir. Dis.* 1984; **130**:663–673.

74. M. Ono, K. Arakawa, M. Mori, T. Sugimoto, and H. Harashima, Separation of fine crackles from vesicular sounds by a nonlinear digital filter. *IEEE Trans. Biomed. Eng.* 1989; **36**(2):286–291.

75. L. J. Hadjileontiadis and S. M. Panas, Nonlinear separation of crackles and squawks from vesicular sounds using third-order statistics. Proc. 18th Annu. Int. Conf. IEEE/EMBS 1996: 2217–2219.

76. L. J. Hadjileontiadis and S. M. Panas, Separation of discontinuous adventitious sounds from vesicular sounds using a wavelet-based filter. *IEEE Trans. Biomed. Eng.* 1997; **44**(12):1269–1281.

77. Y. A. Tolias, L. J. Hadjileontiadis, and S. M. Panas, A fuzzy rule-based system for real-time separation of crackles from vesicular sounds. Proc. 19th Annu. Int. Conf. IEEE/EMBS. 1997: 1115–1118.

78. Y. A. Tolias, L. J. Hadjileontiadis, and S. M. Panas, Real-time separation of discontinuous adventitious sounds from vesicular sounds using a fuzzy rule-based filter. *IEEE Trans. Biomed. Eng.* 1998; **2**(3):204–215.

79. S. Chen, C. F. N. Cowan, and P. M. Grant, Orthogonal least squares learning algorithm for radial basis functions network. *IEEE Trans. Neural Networks* 1991; **2**:302–309.

80. P. A. Mastorocostas, Y. A. Tolias, J. B. Theocharis, L. J. Hadjileontiadis, and S. M. Panas, An orthogonal least squares-based fuzzy filter for real-time analysis of lung sounds. *IEEE Trans. Biomed. Eng.* 2000; **47**(9):1165–1176.

81. L. J. Hadjileontiadis, Y. A. Tolias, and S. M. Panas, Intelligent system modeling of bioacoustic signals using advanced signal processing techniques. In: C. T. Leondes, ed., *Intelligent Systems: Technology and Applications,* vol. 3. Boca Raton, FL: CRC Press, 2002, pp. 103–156.

82. L. J. Hadjileontiadis and I. T. Rekanos, Detection of explosive lung and bowel sounds by means of fractal dimension. *IEEE Signal Proc. Lett.* 2003; **10**(10):311–314.

83. J. Hoevers and R. G. Loudon, Measuring crackles. *Chest* 1990; **98**:1240–1243.

84. L. Cohen, Generalized phase-space distribution function. *J. Math. Phys.* 1966; **7**:781–786.

85. W. J. Williams and J. Jeong, Reduced interference time-frequency distributions. In: B. Boashash, ed., *Time-Frequency Signal Analysis Methods and Applications*. New York: Longman and Cheshire/Wiley Halsted Press, 1992, pp. 75–97.

86. W. J. Williams, Reduced interference distributions: biological applications and interpretations. *Proc. IEEE* 1996; **84**(9): 1264–1280.

87. S. E. Widmalm, W. J. Williams, and C. Zheng, Time frequency distributions of TMJ sounds. *J. Oral Rehab.* 1991; **18**:403–412.

88. S. E. Widmalm, P. L. Westesson, S. L. Brooks, M. P. Hatala, and D. Paesani, Temporomandibular joint sounds: correlation to joint morphology in fresh autopsy specimens. *Amer. J. Orthodont. Dentofac. Orthoped.* 1992; **101**:60–69.

89. J. C. Wood and D. T. Barry, Radon transformation of time-frequency distributions for analysis of multicomponent signals. *IEEE Trans. Signal Proc.* 1994; **42**(11):3166–3177.

90. J. C. Wood and D. T. Barry, Time-frequency analysis of the first heart sound. *IEEE Eng. Med. Biol. Mag.* 1995; **14**(2): 144–151.

91. J. C. Wood et al. Differential effects of myocardial ischemia on regional first heart sound frequency. *J. Appl. Physiol.* 1994; **36**(1):291–302.

92. J. C. Wood and D. T. Barry, Time-frequency analysis of skeletal muscle and cardiac vibrations. *Proc. IEEE* 1996; **84**(9): 1281–1294.

93. Z. Guo, L.-G. Durand, and H. C. Lee, Comparison of time-frequency distribution techniques for analysis of simulated Doppler ultrasound signals of the femoral artery. *IEEE Trans. Biomed. Eng.* 1994; **41**:332–342.

94. Z. Guo, L.-G. Durand, and H. C. Lee, The time-frequency distributions of nonstationary signals based on a Bessel kernel. *IEEE Trans. Signal Proc.* 1994; **42**:1700–1707.

95. V. K. Iyer, P. A. Ramamoorthy, and Y. Ploysongsang, Autoregressive modeling of lung sounds: characterization of source and transmission. *IEEE Trans. Biomed. Eng.* 1989; **36**(11): 1133–1137.

96. L. J. Hadjileontiadis and S. M. Panas, Autoregressive modeling of lung sounds using higher-order statistics: Estimation of source and transmission. In: A. Petropulu, ed., Proc. IEEE Signal Processing Workshop on Higher-Order Statistics '97 (SPW-HOS '97), Banff, Alberta, Canada: IEEE Signal Processing Society, 1997, pp. 4–8.

97. C. L. Nikias and A. P. Petropulu, *Higher-Order Spectra Analysis: A Nonlinear Signal Processing Framework,* 1st ed. Englewood Cliffs, NJ: Prentice-Hall, 1993, chaps. 1–2.

98. A. Swami, J. M. Mendel, and C. L. Nikias, *Higher-Order Spectral Analysis Toolbox*, 3rd ed. Natick, MA: The Mathworks, 1998, chap. 1.

99. L. J. Hadjileontiadis, Analysis and processing of lung sounds using higher-order statistics-spectra and wavelet transform, Ph.D. dissertation, Aristotle University of Thessaloniki, Thessaloniki, Greece, 1997, pp. 139–175.

100. C. L. Nikias and M. Shao, *Signal Processing with Alpha-Stable Distributions and Applications,* 1st ed. New York: Wiley & Sons, 1995, chaps. 1–7.

101. W. Feller, *An Introduction to Probability Theory and Its Applications*, vol. 2. New York: Wiley & Sons, 1996.

102. L. J. Hadjileontiadis and S. M. Panas, On modeling impulsive bioacoustic signals with symmetric α-Stable distributions: application in discontinuous adventitious lung sounds and explosive bowel sounds. Proc. 20th Annu. Int. Conf. IEEE/EMBS, 1998: 13–16.

103. J. H. McCulloch, Simple consistent estimators of stable distribution parameters. *Commun. Statist. Simula.* 1986; **15**(4):1109–1136.

104. I. A. Koutrouvelis, An iterative procedure for the estimation of the parameters of stable laws. *Commun. Statist. Simula.* 1981; **10**(1):17–28.

105. S. K. Chowdhury and A. K. Majumder, Digital spectrum analysis of respiratory sound. *IEEE. Trans. Biomed. Eng.* 1981; **28**(11):784–788.